Biochemistry

© Copyright 1996 by the American Chemical Society Volume 35, Number 20 May 21, 1996

Accelerated Publications

Heat and Cold Denatured States of Monomeric λ Repressor Are Thermodynamically and Conformationally Equivalent†

Guewha S. Huang‡ and Terrence G. Oas*

Department of Biochemistry, Duke University Medical Center, Durham, North Carolina 27710

Received February 1, 1996; Revised Manuscript Received March 27, 1996⊗

ABSTRACT: Although the denaturation of proteins by low temperatures is a well-documented phenomenon, little is known about the molecular details of the process. In this study, the parameters describing the denaturation thermodynamics of residues 6−85 of the N-terminal domain of λ repressor have been determined by fitting the three-dimensional thermal-urea denaturation surface obtained by circular dichroism. The shape of the surface shows cold denaturation at low temperatures and urea concentrations above 2 M, which allows accurate determination of the apparent heat capacity of denaturation (ΔC_p). Denaturation curves based on aromatic ^{1}H NMR spectra give identical denaturation curves, confirming purely two-state folding under all conditions studied. The denaturation surface can be fit with constant ΔC_p and $\delta \ln K_D/\delta$[urea] (K_D is the equilibrium constant for denaturation), consistent with a thermodynamically invariant denatured state. In addition, the aromatic ^{1}H NMR spectrum of the cold denatured state at 0 °C in 3 M urea is essentially identical to the spectrum at 70 °C in 3 M urea. These observations indicate that the structures of the cold and heat denatured states, in the presence of 3 M urea, are thermodynamically and conformationally equivalent.

Structural characterization of partially folded proteins has incited much recent interest (Neri et al., 1992; Alexandrescu et al., 1993, 1994; Van Dael et al., 1993; Arcus et al., 1994; Logan et al., 1994; Lumb & Kim, 1994; Ferrer et al., 1995). These studies' significance must be judged in terms of the relative population of the species under investigation. This is particularly true when the rapid interconversion of different conformations can cause averaging of spectroscopic probes such as nuclear Overhauser effects (NOE's) in nuclear magnetic resonance (NMR)[1] spectra. Because a given species' relative thermodynamic stability determines its population under equilibrium conditions, the first step in any structural investigation of protein folding mechanism should be the determination of folding thermodynamics. The fully

† This work was supported by grants from the American Cancer Society (JFRA-398) and the National Institutes of Health (GM45322).

* To whom correspondence should be addressed: Box 3711; oas@bchm.biochem.duke.edu; (919) 684-4363; (919) 684-8885 (FAX).

‡ Present address: Division of Structural Biology, Institute of Biomedical Sciences, Academia Sinica, Taipei, Taiwan R.O.C.

⊗ Abstract published in *Advance ACS Abstracts*, May 1, 1996.

[1] Abbreviations: CD, circular dichroism spectropolarimetry; EDTA, ethylenediaminetetraacetic acid; HPLC, high-performance liquid chromatography; IPTG, isopropyl β-D-thiogalactopyranoside; NMR, nuclear magnetic resonance spectroscopy; F_D, fraction denatured; R, universal gas constant; T_m, the temperature at which the denatured population equals the native population; TMSP, 3-(trimethylsilyl)propionic acid sodium salt; δ, chemical shift; ΔC_p, heat capacity of denaturation; K_D, equilibrium constant for denaturation; ΔG_D, free energy of denaturation; ΔG_D°, ΔG_D in the absence of denaturant; m, $\delta\Delta G_D/\delta$[urea] or the slope of ΔG_D vs [urea]; T_g, high temperature at which $\Delta G_D^\circ = 0$; T'_g, low temperature at which $\Delta G_D^\circ = 0$; ΔH_g, enthalpy of denaturation at T_g; $\Delta H'_g$, enthalpy of denaturation at T'_g; ΔS_g, entropy of denaturation at T_g; T_h, temperature at which $\Delta H_{Dg} = 0$; T_s, temperature at which the entropy of denaturation is zero or the temperature of maximum stability; λ_{6-85}, residues 6−85 of λ repressor with the replacement of Pro6 by Ser and Tyr85 by Arg; NOESY, nuclear Overhauser enhancement and exchange spectroscopy.

S0006-2960(96)00250-4 CCC: $12.00 © 1996 American Chemical Society

denatured state of a protein is particularly challenging to study by structural methods. In the absence of persistent residual structure, the number of structural probes is limited. NMR chemical shifts, however, are highly sensitive probes of the average local environment of a residue (Perkins & Wüthrich, 1980; Wüthrich, 1986). This sensitivity has been exploited to detect very low populations of folded structure and is therefore useful for qualitative comparison of denatured states (Ropson & Frieden, 1992; Kemmink et al., 1993; Saab-Rincon et al., 1993; Stockman et al., 1993; Van Dael et al., 1993; Celda et al., 1995; Kemmink & Creighton, 1995; Oldfield, 1995).

λ repressor is encoded by the bacteriophage λ *cI* gene and binds to DNA as a dimer (Sauer et al., 1990). The crystal structure for the first 92 residues of the N-terminal domain in both its free and DNA-bound forms is known (Pabo & Lewis, 1982; Jordan & Pabo, 1988; Beamer & Pabo, 1992). The protein consists of five helices that form a single hydrophobic core. Another version of the N-terminal domain, comprising residues 1−102, has been used in genetic protein folding studies and has been characterized with a variety of altered hydrophobic cores. The version of λ repressor used here, λ_{6-85}, comprises residues 6−85 and lacks the dimerization interface (the C-terminal half of helix 5) (Pabo & Lewis, 1982) and the first five amino acids, which are disordered in the free protein (Jordan & Pabo, 1988). The chemical shifts of ^{1}H, ^{15}N, and backbone ^{13}C NMR resonances in the native state and the aromatic side-chain protons in the denatured state have been previously assigned (Huang & Oas, 1995a). Under these conditions the molecule is purely monomeric. NMR and circular dichroism (CD) studies of λ_{6-85} thermal and urea denaturation show that the completely denatured state is the only non-native state populated at temperatures above 25 °C. The solution structure of native λ_{6-85} is very similar to the crystal structure of the λ_{1-92} dimer bound to DNA. The denatured state has a ^{1}H NMR spectrum with random coil chemical shifts, which indicates a completely unfolded structure. The similarity between the aromatic ^{1}H NMR spectra of the thermally denatured state and the urea denatured state at 37 °C indicates that they are identical (Huang & Oas, 1995a). Here we exploit the two-state folding behavior of λ_{6-85} to determine the parameters that completely define its folding thermodynamics.

MATERIALS AND METHODS

Protein Expression and Purification. Plasmid pWL300 containing the gene encoding residues 6−85 of λ repressor cloned into the T7 expression vector (Studier et al., 1990) pAED4 (Doering, 1992) was the generous gift of Wendell Lim. For a typical 1 L scale preparation, the gene was expressed in *Escherichia coli* strain BL21(DE3), induced with 0.4 mM IPTG. The purification protocol is a modification of one used previously for other versions of λ repressor (Lim et al., 1992). The cell lysate (in 40 mL of TE, pH 8.0), from a French press, was loaded onto a 60 mL DEAE-Sephacel (Pharmacia) column equilibrated with 50 mM KCl, 10 mM Tris (pH 8.0), 2 mM $CaCl_2$, 0.1 mM EDTA, and 5% glycerol. The flow-through was dialyzed against 10 mM KCl, 20 mM potassium acetate, pH 5.0, and 5% glycerol using Spectra/Por dialysis tubing. The dialysate was applied to a 15 mL Affigel blue (Bio-Rad) column equilibrated with the same buffer and was eluted with a linear 10−200 mM KCl gradient. The major peak, as detected by absorbance at 229 nm, was further purified by reverse phase HPLC with a C-18 column (Vydac) in acetonitrile/water/0.1% trifluoroacetic acid.

CD Spectroscopy. All CD experiments were conducted with an Aviv 62DS spectropolarimeter equipped with an automated five cell rotary thermoelectric sample holder using 1 mm path-length cells. Samples in 0, 1.0, 2.1, 3.1, and 3.9 M urea consisted of 100 μM protein in a buffer composed of 100 mM NaCl, 20 mM KD_2PO_4, and 99% D_2O, pH 8.0. Protein concentrations were determined by the method of Edelhoch, and urea concentrations were determined by refractometry using the method of Pace (1986). The CD signal was monitored at 222 nm with a bandwidth of 1.5 nm. Data were collected in 1 °C steps with an averaging time of 15 s and an equilibration delay of 30 s. Separate reversibility studies indicate >90% reversibility over the temperature and urea concentration ranges studied.

NMR Spectroscopy. NMR experiments were conducted in the same buffer used for CD studies. Protein and urea concentrations were determined as described above. Proton NMR spectra were collected with automated temperature incrementation as described previously, using a 600 MHz Varian UNITY NMR spectrometer housed in the Duke University NMR Spectroscopy Center. Two-dimensional chemical exchange spectra were collected at 13 mixing times between 10 and 500 ms using a standard 2D NOESY pulse sequence with presaturation of water. NMR data was processed using FELIX 2.3 (Biosym, Inc.).

Denaturation Surface Fitting. The CD denaturation surface was fitted using the Splus statistical package (Statistical Science, Inc.) on a Silicon Graphics 4D/25 workstation. Parameter uncertainties were determined by Monte Carlo sampling of the χ^2 surface (Kaderman & Bates, 1990).

Chemical Exchange Data Fitting. Cross-peak and autopeak volumes were determined as a function of mixing time using FELIX 2.3 (Biosym, Inc.). Autopeak volumes as a function of mixing time were fit as described by Farrow et al. (1994). The exchange cross-peak volumes were fit as ratios to the autopeak having the same indirectly detected frequency (D1 in Figure 4A).

RESULTS AND DISCUSSION

Denaturation Surface Analysis. Numerous thermodynamic studies of protein folding have illuminated the parameters necessary for the complete thermodynamic description of protein folding (Privalov, 1979; Becktel & Schellman, 1987; Pace, 1990; Freire et al., 1992; Scholtz, 1995). These parameters are the number of species and the enthalpy, entropy, and heat capacity of each species relative to a reference state (usually the native state). Under favorable conditions, these parameters can be determined either spectroscopically or calorimetrically, but they are usually difficult to determine under a single set of buffer conditions because the apparent denaturation curve can be equally well fitted with a wide range of ΔC_p values. Fortunately, it is often possible to use pH or a chemical denaturant to produce a series of denaturation curves that can be analyzed in aggregate to produce accurate estimates of the parameters listed above (Privalov, 1979). Spectroscopic observation of cold denaturation is particularly useful because it can only be observed if there is a non-zero denaturation heat capacity

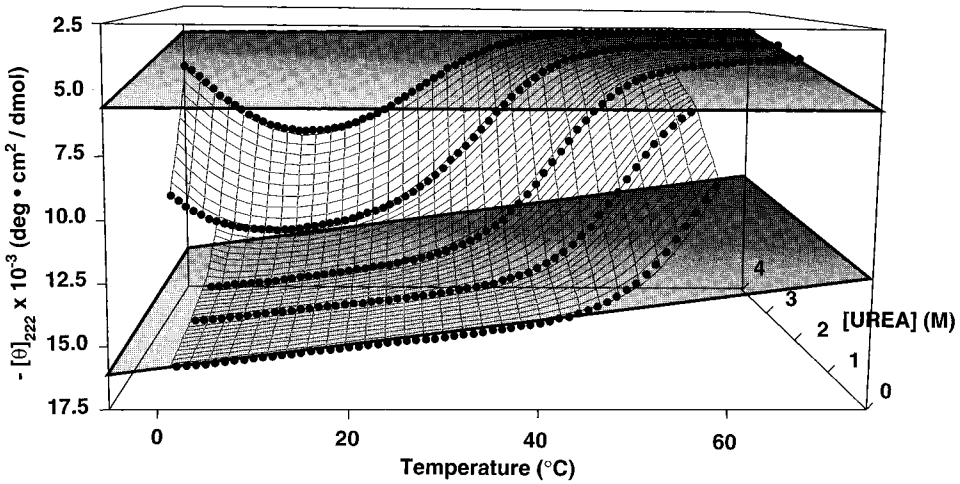

FIGURE 1: Three-dimensional denaturation surface of λ_{6-85} detected by circular dichroism (mean residue ellipticity at 222 nm) under conditions described in Materials and Methods. The ● symbols represent observed data and the gray planes are the fitted native (bottom) and denatured (top) base planes obtained from least squares fitting of the data to eqs 2−7. The slopes and intercepts of the native and denatured base planes are $\theta_N^\circ = -15\,900 \pm 40$ and $\theta_D^\circ = -5600 \pm 100$ deg·cm^{2}dmol^{-1}; $C_N^T = 50 \pm 1$ and $C_D^T = 1 \pm 2$ deg·cm^{2}dmol^{-1} K^{-1};$C_N^U = 220 \pm 20$ and $C_D^U = 460 \pm 20$ deg·cm^2 dmol^{-1} M^{-1}.

(ΔC_p). Thus, the process of fitting the cold denaturation portion of a complete denaturation curve gives an accurate estimate of ΔC_p.

Scholtz compared a variety of approaches for extracting the cardinal thermodynamic parameters from combined thermal and chemical denaturation data (Scholtz, 1995). Here we use the global fitting method described in that study. The method involves fitting the three-dimensional surface for the CD signal at 222 nm versus temperature and urea concentration to a function of 10 parameters (see Figure 1). The two-state denaturation reaction can be written as

$$N \rightleftharpoons D \tag{1}$$

The equilibrium constant for denaturation, K_D, is [D]/[N], where N is the native state and D is the denatured state. K_D is a function of temperature and urea concentration:

$$K_D(T,[U]) = e^{-\Delta G(T,[U])/RT} \tag{2}$$

where R is the universal gas constant, T is the absolute temperature, and [U] is urea concentration. The denaturation free energy, ΔG_D, is

$$\Delta G_D(T,[U]) = \Delta G_D^\circ(T) - m[U] \tag{3}$$

where $\Delta G_D^\circ(T)$ is the denaturation free energy in the absence of urea and is (Becktel & Schellman, 1987)

$$\Delta G_D^\circ(T) = \Delta H_g\left(1 - \frac{T}{T_g}\right) - \Delta C_p\left[(T_g - T) + T\ln\left(\frac{T}{T_g}\right)\right] \tag{4}$$

The four thermodynamic parameters in eqs 2−4 are m, $\delta\Delta G/\delta[U]$; T_g, the upper temperature at which ΔG_D° is 0; ΔH_g, the enthalpy of denaturation at T_g; and ΔC_p, the denaturation heat capacity. In our analysis we assume that m is temperature invariant and ΔC_p is temperature and urea invariant over the range of conditions used. Under favorable conditions, calorimetric data have been interpreted in terms of a relatively small temperature dependence of urea binding (m) and ΔC_p (Privalov et al., 1989; Makhatadze & Privalov, 1992). The molecular basis of these dependencies is not well understood and may vary considerably from protein to protein. Least squares fitting analysis of the temperature coefficients of m and ΔC_p is equivalent to computing the third derivative of the signal with respect to temperature, a process that clearly exceeds the information content of the data. The simplified description we have employed has also been used by other workers (Pace, 1986; Chen & Schellman, 1989; Scholtz, 1995) and is consistent with the observation that λ_{6-85} folds in a two-state fashion under all conditions (see below). Because of the simplification, we refer to the fitted parameter estimates as apparent values.

The remaining six parameters necessary to fit a two-state denaturation surface are the slopes and intercepts of the *planes* that describe the urea and temperature dependence of the native and denatured state CD signals. We refer to these planes as the native and denatured base planes. They are analogous to the base lines used for analysis of conventional two-dimensional denaturation curves (Pace, 1990). The function that describes the complete urea and temperature dependence of the CD signal (Figure 1) is

$$\theta(T,[U]) = \frac{\theta_N(T,[U]) + \theta_D(T,[U])K_D(T,[U])}{1 + K_D(T,[U])} \tag{5}$$

The base planes θ_N(T,[U]) and $\theta_D(T,[U])$ are given by

$$\theta_N(T,[U]) = \theta_N^\circ + C_N^T T + C_N^U[U] \tag{6}$$

and

$$\theta_D(T,[U]) = \theta_D^\circ + C_D^T T + C_D^U[U] \tag{7}$$

where θ_N° and θ_D° are the intercepts of the native and denatured base planes and C_N^T, C_N^U, C_D^T, and C_D^U are the temperature and urea slopes of the native and denatured base planes, respectively.

Figure 1 depicts the best-fit base planes obtained from these parameters. The utility of these base planes lies in the fact that they can be obtained from regions of the thermochemical denaturation surface that are experimentally accessible, i.e., in the low temperature−low urea quadrant

Table 1: Globally Fitted Thermodynamic Parameters for λ_{6-85}

parameter[a]	value[b]	determination method[c]
temperature and denaturant invariant parameters		
m	1.13 ± 0.02 kcal mol^{-1} M^{-1}	nonlinear least squares fit
ΔC_p	1.44 ± 0.03 kcal mol^{-1} K^{-1}	nonlinear least squares fit
heat denaturation		
T_g	57.2 ± 0.1 °C	nonlinear least squares fit
ΔH_g	68 ± 1 kcal mol^{-1}	nonlinear least squares fit
cold denaturation		
T'_g	-16.2 ± 1.5 °C	$T_g^2/(3T_g - 2T_h)$
$\Delta H'_g$	-35.7 ± 3 kcal mol^{-1}	$\Delta C_p(T'_g - T_h)$
reference temperatures		
T_h	10 ± 1.3 °C	$T_g - \Delta H_g/\Delta C_p$
$T_{s(max)}$	13.2 ± 1.1 °C	$T_g\, e^{-\Delta S_g/\Delta C_p}$
stability		
$\Delta G_D^\circ(13)$(max)	4.6 ± 0.2 kcal mol^{-1}	$\Delta H_g + \Delta C_p(T_s - T_g)$
$\Delta G_D^\circ(25)$	4.3 ± 0.2 kcal mol^{-1}	eqs 2−4
$\Delta G_D^\circ(37)$	3.2 ± 0.2 kcal mol^{-1}	eqs 2−4

[a] Parameter definitions: ΔG_D°, free energy of denaturation in the absence of denaturant; m, $\delta\Delta G_D/\delta$[urea] or the slope of ΔG_D vs [urea]; T_g, high temperature at which $\Delta G_D^\circ = 0$; T'_g, low temperature at which $\Delta G_D^\circ = 0$; ΔH_g, enthalpy of denaturation at T_g; $\Delta H'_g$, enthalpy of denaturation at T'_g; ΔS_g, entropy of denaturation at T_g; T_h, temperature at which $\Delta H_{Dg} = 0$; T_s, temperature at which the entropy of denaturation is zero or the temperature of maximum stability. [b] Uncertainty estimates for fitted parameters are from Monte Carlo sampling of the χ^2 surface (Kaderman & Bates, 1990). The uncertainties of derived parameters have been propagated from the uncertainties of fitted parameters using standard error propagation. [c] Fitted parameters are determined by nonlinear least squares fitting of the 3D denaturation surface. Additional fitted parameters not listed in Table 1 are the slopes and intercepts of the native and denatured baseplanes. Equations for derived parameters are primarily from Privalov (1990).

(where the native protein is most stable) and the moderate temperature−high urea quadrant (where aggregation of the unfolded protein is minimized). The six parameters that determine the base planes are independent, as judged by their covariance in a Monte Carlo analysis of the final fitted equation (Kaderman & Bates, 1990). Their independence indicates that they can be reliably extracted from a 10-parameter fit of the complete denaturation surface.

The best-fit apparent values of the four thermodynamic parameters are listed in Table 1. The error estimates listed in Table 1 are not standard errors, as reported by most nonlinear least squares fitting algorithms, but instead are estimates obtained from Monte Carlo sampling of the χ^2 surface (Kaderman & Bates, 1990). This approach gives more realistic parameter uncertainty estimates when two or more parameters have significant covariance. Also listed in Table 1 are thermodynamic parameters calculated from the fitted apparent values for T_g, ΔH_g, and ΔC_p. These calculated parameters include T_s or T_{max}, the temperature of maximum stability, where $\Delta S = 0$; ΔH and ΔG_D° at T_s; T'_g, the low temperature at which $\Delta G_D^\circ = 0$; and ΔH at T'_g. The calculated values of these parameters rely on the assumption that ΔC_p is constant from T_g to T'_g (57 to −16 °C).

It should be noted that the results listed in Table 1 were obtained using D_2O as a solvent to facilitate comparison with NMR data. On the basis of similar studies in H_2O, we estimate that the primary effect of D_2O is to stabilize the protein by ~0.5 kcal/mol at 37 °C in the absence of denaturant (data not shown). Further studies are underway to better characterize solvent isotope effects on the thermodynamic parameters.

Cold Denaturation. Thermodynamic studies of protein folding have shown that there exists a temperature of maximum stability (T_s or T_{max}) at which a protein is most stable (Brandts, 1964). Cold denaturation under equilibrium conditions was first reported by Jacobsen and Christensen for β-lactoglobulin (Jacobsen & Christensen, 1948) and confirmed by many other studies (Pace & Tanford, 1968; Privalov et al., 1986; Griko et al., 1988; Chen & Schellman, 1989; Privalov, 1990; Tamura et al., 1991a,b). Cold denaturation arises from a large positive ΔC_p and a relatively small ΔH_D upon denaturation. At temperatures above T_{max}, ΔH_D is positive, favoring the native state. However, because ΔC_p is the temperature coefficient of $\Delta H(T)$, ΔH decreases with decreasing temperature. When ΔH drops below zero, denaturation becomes exothermic. Further temperature decreases destabilize the protein and cold denaturation is observed. This phenomenon usually occurs at subzero temperatures, but under destabilizing conditions (i.e., in the presence of denaturant or destabilizing mutations) ΔH is reduced and cold denaturation can be studied at higher temperatures (Privalov, 1990). Calorimetric studies have shown that the primary effect of denaturant is to shift the ΔG_D versus temperature curve vertically, without significantly perturbing the temperature of maximum stability. For this reason, the primary effect of denaturant is to increase the population of denatured molecules, without perturbing the overall temperature dependence of ΔG_D (Privalov, 1990).

Thermodynamic analysis of cold denaturation has been reported for several proteins (Nojima et al., 1977; Cho et al., 1982; Privalov et al., 1986; Griko et al., 1988; Chen & Schellman, 1989; Tamura et al., 1991a). Two general assumptions are used in these studies: that folding is two state and that a single set of parameters can be used to fit both heat and cold denaturation. Two-state folding implies that only the native and denatured states are populated. The extension of thermodynamic parameters from heat denatured states to cold denatured states implies a fundamental similarity between these two states.

As shown in Figure 1, the CD signal of λ_{6-85} at 222 nm indicates a loss of helicity at temperatures below 13 °C in 3 M urea or higher. Loss of helicity is due to denaturation at low temperatures, i.e., cold denaturation. As shown in Figure 2, this conclusion is supported by the temperature dependence of the aromatic ^{1}H NMR spectrum in the presence of 3 M urea.

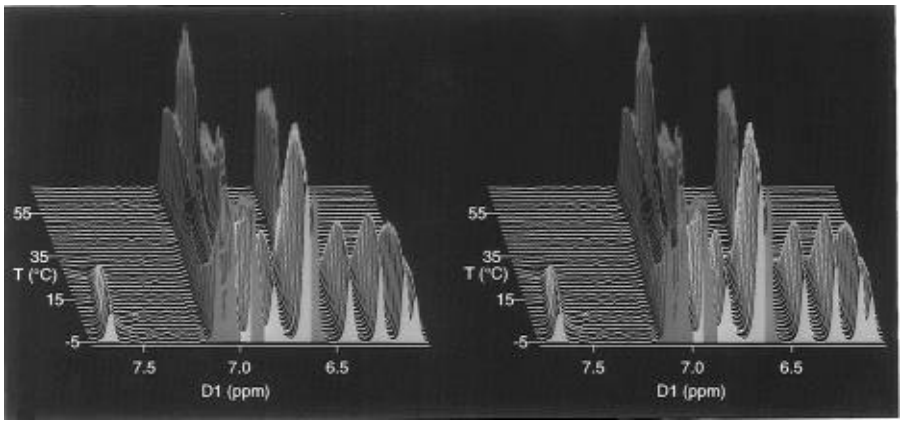

FIGURE 2: Stereoview of the λ_{6-85} aromatic ^{1}H NMR spectrum as a function of temperature in the presence of 3 M urea. Peaks corresponding to the native and denatured states are shown in green and magenta, respectively.

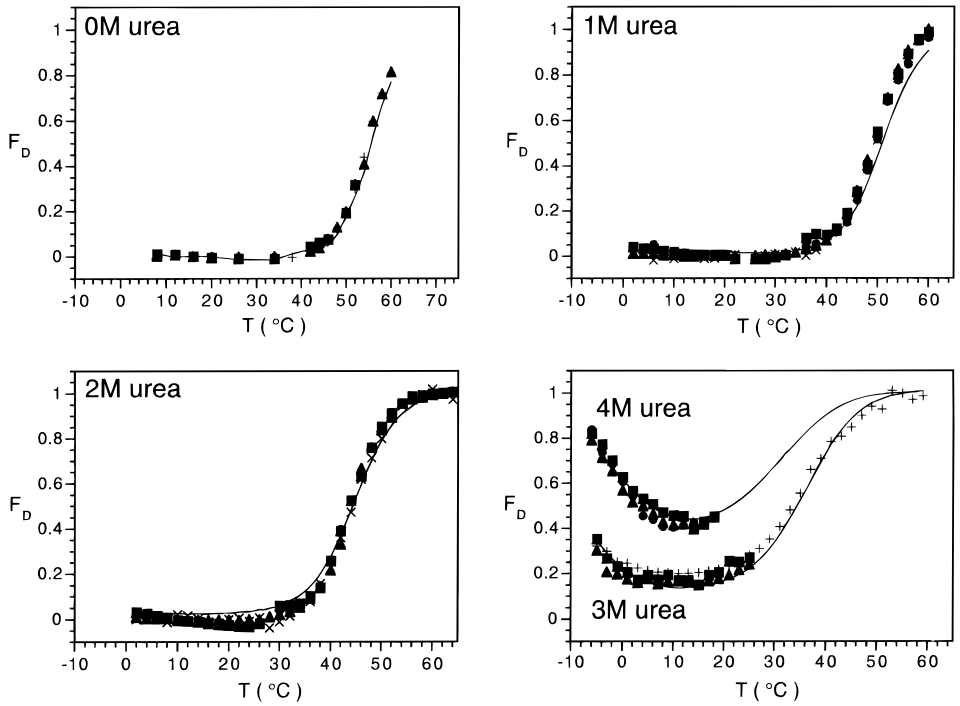

FIGURE 3: Denaturation curves of λ_{6-85} at five concentrations of urea as detected by aromatic ^{1}H chemical shifts and the CD signal at 222 nm. The filled symbols represent F_D calculated from the chemical shifts or intensities of the aromatic ^{1}H resonances of Tyr22 (▲), Phe51 (■), Tyr60 (×), and Phe76 (●). The + symbols are F_D calculated from intensity ratios of resolvable native and denatured peaks in the slow exchange regime. Lines show the results of the least squares fitting of the CD denaturation surface to eqs 2−7.

The λ_{6-85} native and denatured state aromatic proton resonances have been previously assigned and are depicted in green and magenta, respectively, in Figure 2. In 3 M urea, λ_{6-85} folding is slow on the NMR time scale ($<100 s^{-1}$). In this regime, native and denatured state resonances remain sharp at all temperatures and their intensity reflects the fractional population of the corresponding state. The spectra in Figure 2 show evidence for cold denaturation. As the temperature is increased from −5 to +13 °C, the native resonances increase in intensity and then decrease as the temperature is increased above 13 °C (T_{max}).

Two-State Folding. The denaturation curves depicted in Figure 3 show that λ_{6-85} folding is two state under all conditions investigated. We have previously exploited the sensitivity of the aromatic proton chemical shifts to local environment to establish two-state folding under heat denaturation conditions and to measure folding kinetics. We now extend this approach to compare the denaturation curves under cold denaturation conditions. The symbols in Figure 3 show the fraction denatured (F_D) curves obtained from the ^{1}H NMR spectrum of the aromatic residues. Also shown are lines representing F_D obtained from the best fit of the CD denaturation surface. Figure 3 shows that four regions of local tertiary structure (detected by aromatic ^{1}H NMR resonances of Tyr21, Phe51, Tyr60, and Phe76) and the global secondary structure (detected by CD signal at 222 nm) have identical denaturation curves under all conditions. This observation provides particularly strong evidence for two-state folding and strengthens the assumptions that ΔC_p and m are temperature and urea invariant.

Further evidence for two-state folding is found in the slow exchange regime NMR spectra (Figure 2). At all temperatures, the peaks correspond to either native or denatured resonances. There are no detectable peaks at other positions over a temperature range where the cold denatured, native, and heat denatured states are populated. Most significantly, two-state folding under all conditions implies that the heat and cold denatured states of λ_{6-85} are identical.

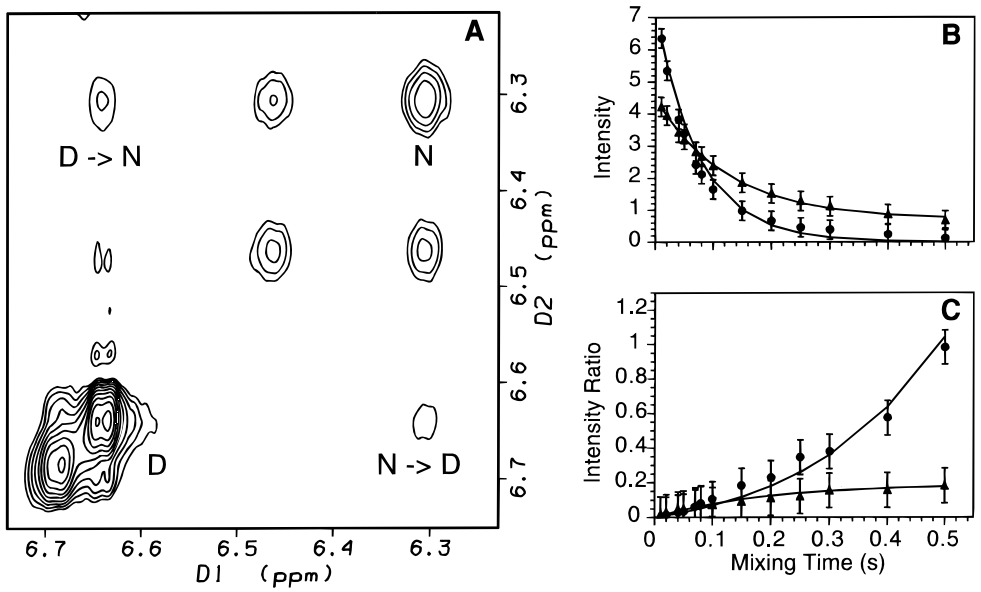

FIGURE 4: (A) Region of the chemical exchange spectrum of λ_{6-85} in 3 M urea at −5 °C depicting the exchange cross peaks between the native and denatured Tyr22 ϵ resonances. (B) Peak intensities vs mixing time: I_{NN} (●) and I_{DD} (▲). (C) Peak ratios vs mixing time: I_{ND}/I_{NN} (●) and I_{DN}/I_{DD} (▲). Lines represent fits to the data using the parameter values $R_{NN} = 12.6\ s^{-1}$, $R_{DD} = 7\ s^{-1}$, $k_f = 1\ s^{-1}$, and $k_u = 0.5\ s^{-1}$.

It is important to note that our use of the term "state" refers to a thermodynamically distinguishable species whose population can be evaluated. Clearly, both the native and denatured states of proteins are ensembles that consist of interconverting substates or conformations (Dill & Shortle, 1991; Wagner, 1995). In seeking to characterize the native and denatured states, we are compelled to describe their average properties, unless distinct subpopulations can be observed and quantified. Thus, the CD and NMR data described in this and previous studies (Huang & Oas, 1995a,b) of λ_{6-85} are consistent with two and only two thermodynamically distinguishable ensembles, which we refer to as the native and denatured states.

Cold Denaturation Kinetics. In the presence of 3 M urea at low temperatures, the folding of λ_{6-85} is slow on the NMR time scale. This means that it is possible to observe peaks arising from both the native and denatured states in the ^{1}H NMR spectrum. Further, the exchange is manifested in cross peaks between native and denatured peaks for the same proton in the two dimensional exchange spectrum (Figure 4A). The cross-peak intensity is a function of the mixing time and the rate of interconversion, which can be obtained by nonlinear least squares fitting of the data in Figure 4B,C (see Materials and Methods). On the basis of this analysis, we conclude that the rate constants for folding and unfolding at −5 °C are $1 \pm 0.5\ s^{-1}$ and $0.5 \pm 0.3\ s^{-1}$, respectively. Folding is ∼200-fold slower than folding measured at 37 °C under the same buffer conditions, corresponding to an Arrhenius activation energy of 20 kcal/mol. However, the Arrhenius treatment assumes that the activation energy is temperature invariant, which is almost certainly not the case in this instance (Oliveberg et al., 1995). Further studies are necessary to characterize fully the temperature dependence of λ_{6-85} folding kinetics.

Comparison of the Heat and Cold Denatured States. Figure 5 shows the aromatic ^{1}H NMR spectra of λ_{6-85} at 0 °C in the presence (Figure 5A) and absence (Figure 5B) of 3 M urea. Figure 5A shows both native and cold denatured peaks. To compare the spectrum of heat and cold denatured λ_{6-85}, we have subtracted the native spectrum (Figure 5B) from the native/cold denatured spectrum (Figure 5A) to obtain a difference spectrum of the cold denatured state (Figure 5A−B). The similarity between the aromatic NMR spectra of the cold and heat (Figure 5C) denatured states is striking. Given the sensitivity of the aromatic chemical shifts to local tertiary structure, these spectra provide strong evidence that the heat and cold denatured states in 3 M urea are identical and completely unfolded. This conclusion differs from those of previous NMR studies of the cold denatured states other proteins. In a recent study of β-lactoglobulin, it was concluded on the basis of ^{1}H spectral characteristics and NOE experiments that the cold denatured state was significantly more compact than that of the heat denatured state (Griko & Kutyshenko, 1994). Another study of *Streptomyces* subtilisin inhibitor (SSI) found a significant difference in the ^{1}H NMR spectra of the cold and heat denatured states (Tamura et al., 1991b). More recently, small-angle X-ray scattering studies have shown that the radius of gyration of heat denatured SSI is 25% larger than cold denatured protein (Konno et al., 1995). These differences may reflect the importance of sequence in determining the average structure, if any, of the denatured state, particularly at temperatures where enthalpic interactions favor denaturation. However, given the importance of solvent in the folding reaction, there is no reason to expect that the heat and cold denatured states must differ. The relative stability of the denatured state at low temperatures is a consequence of a large positive denaturation heat capacity, as it is at high temperatures (Privalov & Makhatadze, 1992; Gomez et al., 1995).

The samples whose cold and heat denatured spectra are compared in parts A−B and C of Figure 5 contained 3 M urea in order to produce observable denatured populations. For this reason, the protein in these samples was denatured by urea in addition to cold and heat. It is possible that the

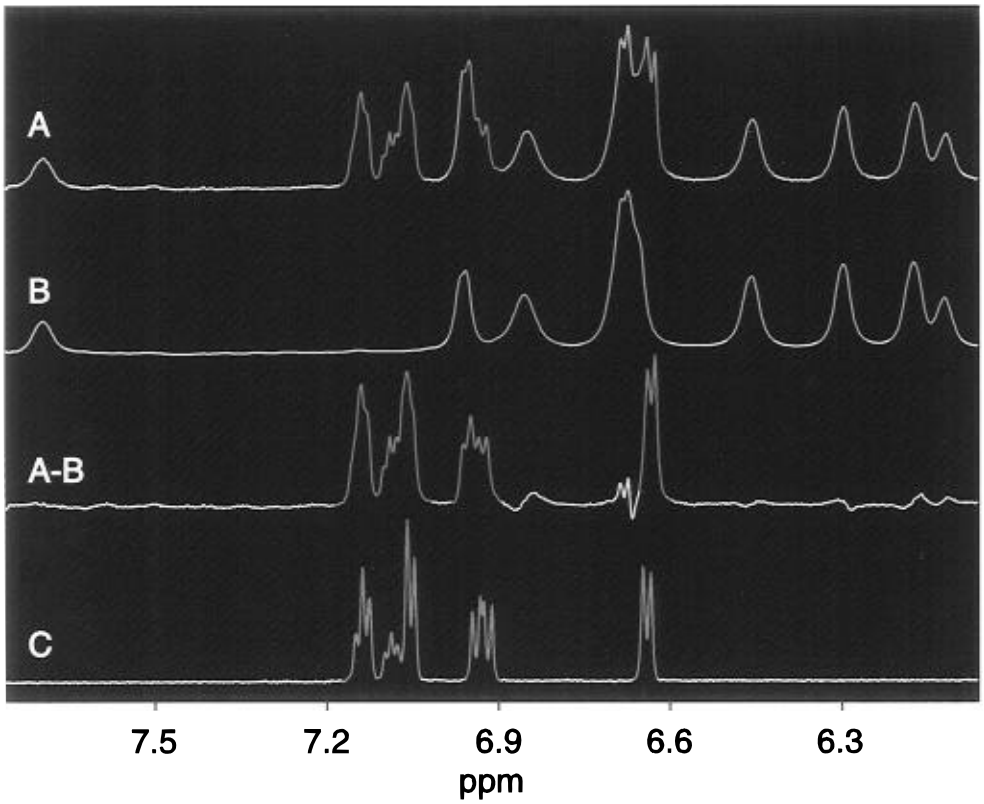

FIGURE 5: Aromatic ^{1}H NMR spectra of the cold and heat denatured states of λ_{6-85}. (A) Partially cold-denatured λ_{6-85} at −5 °C in 3 M urea. B) Fully native λ_{6-85} at 0 °C, 0 M urea. (A−B) Difference spectrum obtained by subtracting spectrum B from spectrum A. Spectrum B was left-shifted and its intensity adjusted to produce optimal removal of native peaks. (C) Fully denatured spectrum at 70 °C in 3 M urea. Peaks corresponding to the native and denatured states are shown in green and magenta, respectively.

similarity between the cold and heat denatured states is due to the presence of urea in both samples. We consider this unlikely on the basis of the thermodynamic data. The denaturation curves obtained from the NMR chemical shifts (0−2 M urea) or relative intensities (3 and 4 M) fit the two-state model very well (see Figure 3). This would not be the case if the spectrum of the cold denatured protein in the presence and absence of urea differed. The temperature of maximum stability is invariant with denaturant in our model, as has been directly observed in other proteins (Privalov, 1990), indicating that the cold denatured states in 0 and 3 M urea are thermodynamically indistinguishable. On this basis, we conclude that the average denatured state conformation is similar in 0 and 3 M urea.

Thermodynamics of λ_{6-85} Denaturation. Dynamic NMR studies of λ_{6-85} folding kinetics show that it folds extremely rapidly (3600 s^{-1} at 37 °C) (Huang & Oas, 1995b). Prior to the present studies, it was plausible that fast folding is initiated from a compact denatured state under the conditions of the experiment, thus avoiding a slow step involving collapse from a more extended denatured conformation (Gittis et al., 1993; Lattman et al., 1994). The thermodynamic parameters in Table 1 can be used to deduce some of the properties of the λ_{6-85} denatured state. On a per residue basis, the apparent ΔC_p and ΔH_D at 25 °C are very similar to values given by Privalov for the average of several other proteins (Privalov, 1979). For this reason, it is unlikely that the denatured state of λ_{6-85} is significantly more compact than the denatured state of these proteins. The parametrization of ΔC_p and ΔH_D as a function of buried polar and nonpolar surface area has been remarkably successful in predicting ΔC_p and ΔH_D for a number of proteins (Gomez et al., 1995). On the basis of our model of the λ_{6-85} solution structure, the predicted ΔC_p and ΔH_D are 1.1 kcal/(mol·K) and 55 kcal/mol, respectively. These values are lower than the observed values listed in Table 1, suggesting that the λ_{6-85} denatured state is, if anything, *less* compact than predicted on the basis of the solvent accessibility of model tripeptides. Thus, the folding thermodynamics under conditions very similar to those of the kinetic studies show that a compact denatured state is unlikely. In summary, the stability, enthalpy, and heat capacity of λ_{6-85} are comparable to other proteins its size lacking disulfide bonds and prosthetic groups. This makes λ_{6-85} a good folding model from a thermodynamic point of view.

CONCLUSIONS

There has been ample experimental demonstration of the phenomenon of cold denaturation (Privalov, 1990; Antonino et al., 1991; Tamura et al., 1991a,b; Griko & Kutyshenko, 1994; Agashe & Udgaonkar, 1995). Additionally, cold denaturation has been seen as the natural thermodynamic consequence of the large denaturation heat capacity increment of proteins (Privalov, 1990). However, a detailed molecular description of cold denaturation has been elusive. Why do low temperatures destabilize proteins? The temperature dependence of denatured state/solvent interactions is generally considered a primary source of the effect (Privalov, 1990; Schiraldi & Pezzati, 1992). This temperature dependence could arise either from a strong temperature effect on the denatured state or from a strong temperature dependence of the properties of water and its interactions with the protein. If the average denatured state structure depends strongly on temperature, its average solvent-aces-

sible surface area might also change. Our data indicate that the aromatic amino acids of λ_{6-85} detect a denatured state environment that is the same at both 0 and 70 °C in 3 M urea. Given the sensitivity of chemical shifts to structural changes, it is unlikely that the average conformation of the denatured protein is grossly different. Thus, the strongly temperature-dependent properties of water itself and the way it interacts with a relatively constant denatured polypeptide are the likely molecular basis of cold denaturation in λ_{6-85}. This conclusion is consistent with previous experimental and theoretical studies of the interaction of water with proteins and small organic molecules (Némethy & Scheraga, 1962; Jorgensen et al., 1985; Finney & Soper, 1994; Kusalik & Svishchev, 1994; Toone, 1994).

We have demonstrated a general method for determining the thermodynamic properties of a protein using both CD and NMR spectroscopic data. Further studies of λ_{6-85} will exploit this method for determining the effect of mutations on the native and denatured states of the molecule. The apparent values of thermodynamic parameters determined in this study indicate that λ_{6-85} is an excellent small protein model for kinetic and thermodynamic investigations of the protein folding reaction.

ACKNOWLEDGMENT

The authors thank Randy Burton, Peggy Daugherty, Tiffany Calderone, and Ron Venters for technical assistance, Wendall Lim for the λ_{6-85} plasmid, Eric Toone for helpful discussion, and Gary Pielak, John Schellman, and Marty Scholtz for constructive comments on the manuscript.

REFERENCES

Agashe, V. R., & Udgaonkar, J. B. (1995) *Biochemistry 34*, 3286−3299.
Alexandrescu, A. T., et al. (1993) *Biochemistry 32*, 1707−1718.
Alexandrescu, A. T., et al. (1994) *Biochemistry 33*, 1063−1072.
Antonino, L. C., et al. (1991) *Proc. Natl. Acad. Sci. U.S.A. 88*, 7715−7718.
Arcus, V. L., et al. (1994) *Proc. Natl. Acad. Sci. U.S.A. 91*, 9412−9416.
Beamer, L. J., & Pabo, C. O. (1992) *J. Mol. Biol. 227*, 177−196.
Becktel, W. J., & Schellman, J. A. (1987) *Biopolymers 26*, 1858−1877.
Brandts, J. F. (1964) *J. Am. Chem. Soc. 86*, 4291−4301.
Celda, B., et al. (1995) *J. Biomol. NMR 5*, 161−172.
Chen, B.-L., & Schellman, J. A. (1989) *Biochemistry 28*, 685−691.
Cho, K. C., et al. (1982) *Biochim. Biophys. Acta 701*, 206−215.
Dill, K. A., & Shortle, D. (1991) *Annu. Rev. Biochem. 60*, 795−825.
Doering, D. S. (1992) Ph.D. Thesis, Massachusetts Institute of Technology, Cambridge, MA.
Farrow, N. A., et al. (1994) *J. Biomol. NMR 4*, 727−734.
Ferrer, M., et al. (1995) *Nat. Struct. Biol. 2*, 211−217.
Finney, J. L., & Soper, A. K. (1994) *Chem. Soc. Rev.*, 1−10.
Freire, E., et al. (1992) *Biochemistry 31*, 250−256.
Gittis, A. G., et al. (1993) *J. Mol. Biol. 232*, 718−724.
Gomez, J., et al. (1995) *Proteins 22*, 404−412.
Griko, Y. V., & Kutyshenko, V. P. (1994) *Biophys. J. 67*, 356−363.
Griko, Y. V., et al. (1988) *J. Mol. Biol. 202*, 127−138.
Huang, G. S., & Oas, T. G. (1995a) *Biochemistry 34*, 3884−3892.
Huang, G. S., & Oas, T. G. (1995b) *Proc. Natl. Acad. Sci. U.S.A. 92*, 6878−6882.
Jacobsen, C. F., & Christensen, L. K. (1948) *Nature (London) 161*, 30−32.
Jordan, S. R., & Pabo, C. O. (1988) *Science 242*, 893−899.
Jorgensen, W. L., et al. (1985) *J. Phys. Chem. 89*, 3470−3473.
Kaderman, E., & Bates, D. (1990) in *Computer Science and Statisitics*, Proceedings of the 22nd Symposium on the Interface, pp 382−386, Springer Verlag, New York.
Kemmink, J., & Creighton, T. E. (1995) *J. Mol. Biol. 245*, 251−260.
Kemmink, J., et al. (1993) *J. Mol. Biol. 230*, 312−322.
Konno, T., et al. (1995) *J. Mol. Biol. 251*, 95−103.
Kusalik, P. G., & Svishchev, I. M. (1994) *Science 265*, 1219−1221.
Lattman, E. E., et al. (1994) *Biochemistry 33*, 6158−6166.
Lim, W. A., et al. (1992) *Biochemistry 31*, 4324−4333.
Logan, T. M., et al. (1994) *J. Mol. Biol. 236*, 637−648.
Lumb, K. J., & Kim, P. S. (1994) *J. Mol. Biol. 236*, 412−420.
Makhatadze, G. I., & Privalov, P. L. (1992) *J. Mol. Biol. 226*, 491−505.
Némethy, G., & Scheraga, H. A. (1962) *J. Phys. Chem. 66*, 1773−1789.
Neri, D., et al. (1992) *Science 257*, 1559−1563.
Nojima, H., et al. (1977) *J. Mol. Biol. 116*, 429−442.
Oldfield, E. (1995) *J. Biomol. NMR 5*, 217−225.
Oliveberg, M., et al. (1995) *Proc. Natl. Acad. Sci. U.S.A. 92*, 8926−8929.
Pabo, C. O., & Lewis, M. (1982) *Nature (London) 298*, 443−447.
Pace, C. N. (1986) *Methods Enzymol. 131*, 266−280.
Pace, C. N. (1990) *Trends Biochem. Sci. 15*, 14−17.
Pace, C. N., & Tanford, C. (1968) *Biochemistry 7*, 198−207.
Perkins, S. J., & Wüthrich, K. (1980) *J. Mol. Biol. 138*, 43−64.
Privalov, P. L. (1979) *Adv. Protein Chem. 33*, 167−241.
Privalov, P. L. (1990) *Crit. Rev. Biochem. Mol. Biol. 25*, 281−305.
Privalov, P. L., & Makhatadze, G. I. (1992) *J. Mol. Biol. 224*, 715−723.
Privalov, P. L., et al. (1986) *J. Mol. Biol. 190*, 487−498.
Privalov, P. L., et al. (1989) *J. Mol. Biol. 205*, 737−750.
Ropson, I. J., &. Frieden, C. (1992) *Proc. Natl. Acad. Sci. U.S.A. 89*, 7222−7226.
Saab-Rincon, G., et al. (1993) *Biochemistry 32*, 13981−13990.
Sauer, R. T., et al. (1990) *Adv. Protein Chem. 40*, 1−61.
Schiraldi, A., & Pezzati, E. (1992) *Thermochim. Acta 199*, 105−114.
Scholtz, J. M. (1995) *Protein Sci. 4*, 35−43.
Stockman, B. J., et al. (1993) *J. Biomol. NMR 3*, 285−296.
Studier, F. W., et al. (1990) *Methods Enzymol. 185*, 60−89.
Tamura, A., et al. (1991a) *Biochemistry 30*, 11313−11320.
Tamura, A., et al. (1991b) *Biochemistry 30*, 11307−11313.
Toone, E. J. (1994) *Curr. Opin. Struct. Biol. 4*, 719−728.
Van Dael, H., et al. (1993) *Biochemistry 32*, 11886−11894.
Wagner, G. (1995) *Nat. Struct. Biol. 2*, 255−257.
Wüthrich, K. (1986) *NMR of Proteins and Nucleic Acids*, Wiley, New York.

BI960250L